
Article:
Mathieu, A.L., Verronese, E., Rice, G.I. et al. (37 more authors) (2015) PRKDC mutations associated with immunodeficiency, granuloma, and autoimmune regulator-dependent autoimmunity. Journal of Allergy and Clinical Immunology, 135 (6). pp. 1578-1588. ISSN 0091-6749

https://doi.org/10.1016/j.jaci.2015.01.040

Elsevier Editorial System(tm) for Journal of Allergy and Clinical Immunology
Manuscript Draft

Manuscript Number: JACI-D-14-00541R3

Title: PRKDC mutations associated with immunodeficiency, granuloma and AIRE-dependent autoimmunity

Article Type: Original Article

Section/Category: Immune Deficiencies, Infection, and Systemic Immune Disorders

Keywords: Autoimmune Regulator (AIRE); Tolerance; DNA-PKcs; PRKDC; autoimmunity; VDJ recombination; Severe combined immunodeficiency; RAG

Corresponding Author: Dr. alexandre belot, MD, PhD

Corresponding Author's Institution: Hospices Civils de Lyon

First Author: Anne-Laure Mathieu, PhD

Order of Authors: Anne-Laure Mathieu, PhD; Estelle Veronese, BS; Gillian I Rice, PhD; Fanny Fouyssac, MD; Yves Bertrand, MD; Capucine Picard, MD; Marie Chansel, MSc; Jolan E Walter, MD, PhD; Luigi D Notarangelo, MD; Manish Butte, MD, PhD; Kari C Nadeau, MD, PhD; Krisztian Csomos, PhD; David J Chen, PhD; Karin Chen, MD; Ana Delgado, BS; Chantal Rigal, BS; Christine Bardin, BS; Catharina Schuetz, MD, PhD; Despina Moshous, MD, PhD; Héloïse Reumaux, MD; François Plenat, MD, PhD; Alice Phan, MD, PhD; Marie-Thérèse Zabot, PharmD, PhD; Brigitte Balme, MD; Sébastien Viel, PharmD; Jacques Bienvenu, PharmD, PhD; Pierre Cochat, MD, PhD; Mirjam van Der Burg, PhD; Christophe Caux, PhD; Helen Kemp, BSc, PhD; Isabelle Rouvet, PharmD, PhD; Christophe Malcus, PharmD, PhD; Jean-François Méritet, PhD; Annick Lim, PhD; Yanick J Crow, MD, PhD; Nicole Fabien, PharmD, PhD; Christine Menetrier-Caux, PhD; Jean-Pierre De Villartay, PhD; Thierry Walzer, PhD; alexandre belot, MD, PhD

Manuscript Region of Origin: FRANCE

Abstract: BackgroundPRKDC encodes for DNA-dependent protein kinase catalytic subunit (DNA-PKcs), a kinase that forms part of a complex (DNA-PK) crucial for DNA double-strand break (DSB) repair and V(D)J recombination. In mice, DNA-PK also interacts with the transcription factor AIRE (autoimmune regulator) to promote central T cell tolerance. ObjectiveWe sought to understand the causes of an inflammatory disease with granuloma and autoimmunity, associated with decreasing T and B cell counts over time diagnosed in two unrelated patients.MethodsGenetic, molecular, and functional analyses were performed to characterize an inflammatory disease evocative of a combined immunodeficiency.Results We identified PRKDC mutations in both patients. These patients exhibited a defect in DNA DSB repair and V(D)J recombination. Whole blood mRNA analysis revealed a strong interferon signature. Upon activation, memory T cells displayed a skewed cytokine response typical of Th2 and Th1 but not Th17. Moreover, mutated DNA-PKcs failed to promote AIRE-dependent transcription of peripheral tissue antigens in vitro. The latter defect correlated in vivo with the production of anti-Calcium Sensing Receptor (anti-CaSR) autoantibodies, which are typically found in AIRE-deficient patients. In addition, 9 month after bone marrow transplantation, Patient 1 developed Hashimoto thyroiditis suggesting that organ-specific autoimmunity may be linked to non-hematopoietic cells such as AIRE-expressing thymic epithelial cells.ConclusionDeficiency of DNA-PKcs,

a key AIRE partner, can present as an inflammatory disease with organ-specific autoimmunity, thus suggesting a role for DNA-PKcs in regulating autoimmune responses and maintaining AIRE-dependent tolerance in humans.

PRKDC mutations associated with immunodeficiency, granuloma and AIRE-dependent autoimmunity

Anne-Laure Mathieu, PhD,[1,2,3,4], Estelle Veronese, BS,[5], Gillian I. Rice, PhD,[6], Fanny Fouyssac, MD,[7], Yves Bertrand, MD, PhD,[8], Capucine Picard, MD, PhD[9], Marie Chansel, MSc,[10], Jolan E. Walter, MD, PhD[11], Luigi D. Notarangelo,MD[12], Manish Butte, MD, PhD[13], Kari Christine Nadeau, MD, PhD,[13], Krisztian Csomos, PhD,[11], David J. Chen, PhD,[14], Karin Chen, MD,[15], Ana Delgado, BS,[5], Chantal Rigal, BS,[5], Christine Bardin, BS,[5], Catharina Schuetz, MD, PhD[16], Despina Moshous, MD, PhD[10], Héloïse Reumaux, MD,[17], François Plenat, MD, PhD[18], Alice Phan, MD, PhD,[22], Marie-Thérèse Zabot, PharmD, PhD,[20], Brigitte Balme, MD,[19], Sébastien Viel, PharmD[1,2,3,4,21] Jacques Bienvenu, PharmD, PhD,[1,2,3,4,21], Pierre Cochat, MD, PhD,[22], Mirjam Van Der Burg, PhD,[23], Christophe Caux, PhD[5], Helen Kemp, BSc, PhD,[24], Isabelle Rouvet, PharmD, PhD[20], Christophe Malcus, PharmD, PhD,[25], Jean-Francois Méritet, PharmD, [26], Annick Lim, PhD,[27], Yanick J. Crow, MD, PhD[6], Nicole Fabien, PharmD, PhD[21], Christine Menetrier-Caux, PhD[5], Jean-Pierre De Villartay, PhD[10], Thierry Walzer, PhD[1,2,3,4], Alexandre Belot, MD, PhD[1,2,3,4,22]

[1]CIRI, International Center for Infectiology Research, Université de Lyon,
[2]Inserm, U1111,
[3]Ecole Normale Supérieure de Lyon,
[4]CNRS, UMR5308, Lyon, France.
[5]Université de Lyon, INSERM U1052, Centre de Recherche en Cancérologie de Lyon; Plateforme d'Innovation en Immuno-monitoring et Immunothérapie, Centre Léon Bérard; LabEx DEVweCAN, Lyon, France.
[6]Manchester Centre for Genomic Medicine, Institute of Human Development, Faculty of Medical and Human Sciences, Manchester Academic Health Centre, Manchester, UK.

[7]Pediatric haematology and oncology department, children hospital - CHU NANCY Vandoeuvre les Nancy, France.
[8]Institut d'Hématologie et d'Oncologie Pédiatrique (Hospices Civils de Lyon), Université Claude Bernard Lyon I, Lyon, France.
[9]Study Center for Primary Immunodeficiencies, Assistance Publique-Hôpitaux de Paris, Necker Hospital, Laboratory of Human Genetics of Infectious Diseases, Necker Branch, INSERM U1163, Sorbonne Paris Cité, Paris Descartes University, Imagine Institute, Paris Descartes University, Paris, France.
[10]INSERM UMR 1163, Laboratoire Dynamique du Génome et Système Immunitaire Université Paris Descartes - Sorbonne Paris Cité, , Imagine Institute, Paris.
[11]Pediatric Allergy&Immunology and the Center for Immunology and Inflammatory Diseases, Massachusetts General Hospital *for* Children, Harvard Medical School, Boston, MA, USA.
[12]Division of Immunology, Boston Children's Hospital and Harvard Medical School, Boston, MA 02115, USA.
[13]Department of Pediatrics, Division of Allergy, Immunology, Rheumatology, Stanford University, Stanford, CA USA.
[14]Division of Molecular Radiation Biology Department of Radiation Oncology, The University of Texas Southwestern Medical Center Dallas, TX 75390, USA.
[15]Department of Pediatrics, Division of Allergy, Immunology & Rheumatology, University of Utah School of Medicine Salt Lake City, Utah, USA.
[16]Department of Pediatrics and Adolescent Medicine, University Medical Center Ulm, Germany.
[17]Pediatric Rheumatology and Emergency Unit, Jeanne de Flandre Hospital, Lille, France.
[18]Pathology Department: Hémato-Oncologie Pédiatrique. CHU Nancy, France
[19]Pathology Department, Centre Hospitalier Lyon Sud, Hospices Civils de Lyon, France.
[20] Biotechnology Department, Hospices Civils de Lyon, Lyon, France.
[21]Immunobiology Department, Hospices Civils de Lyon, Centre Hospitalier Lyon Sud, France.
[22]Pediatric Rheumatology, Nephrology and Dermatology Department and EPICIME Hospices Civils de Lyon and Université Claude-Bernard Lyon 1, Lyon, France.

[23]Deptartment of Immunology, Erasmus MC, University Medical Center Rotterdam, Rotterdam, the Netherlands.
[24]Department of Human Metabolism The Medical School University of Sheffield Sheffield, UK.
[25] Cell Immunology department, Hopital Edouard Herriot, Hospices Civils de Lyon, Hôpital Edouard Herriot, Lyon, France.
[26]Virology Unit, Hopital Cochin, Assistance Publique-Hôpitaux de Paris, Paris, France
[27]Immunoscope group, Immunology Department, Institut Pasteur, Paris, France

Address correspondence to:

Dr. Alexandre Belot, MD, PhD

Service de Néphrologie, Rhumatologie, Dermatologie Pédiatriques, Hôpital Femme Mère Enfant, Hospices Civils de Lyon, 57 Bd Pinel, 69677 BRON cedex, FRANCE

Tel: 00 33 4 72 85 64 81

Fax: 00 33 4 72 85 67 68

Email: alexandre.belot@chu-lyon.fr

Conflict of interest: The authors have declared that no conflict of interest exists.

Abstract

Background

PRKDC encodes for DNA-dependent protein kinase catalytic subunit (DNA-PKcs), a kinase that forms part of a complex (DNA-PK) crucial for DNA double-strand break (DSB) repair and V(D)J recombination. In mice, DNA-PK also interacts with the transcription factor AIRE (autoimmune regulator) to promote central T cell tolerance.

Objective

We sought to understand the causes of an inflammatory disease with granuloma and autoimmunity, associated with decreasing T and B cell counts over time diagnosed in two unrelated patients.

Methods

Genetic, molecular, and functional analyses were performed to characterize an inflammatory disease evocative of a combined immunodeficiency.

Results

We identified *PRKDC* mutations in both patients. These patients exhibited a defect in DNA DSB repair and V(D)J recombination. Whole blood mRNA analysis revealed a strong interferon signature. Upon activation, memory T cells displayed a skewed cytokine response typical of Th2 and Th1 but not Th17. Moreover, mutated DNA-PKcs failed to promote AIRE-dependent transcription of peripheral tissue antigens *in vitro*. The latter defect correlated *in vivo* with the production of anti-Calcium Sensing Receptor (anti-CaSR) autoantibodies, which are typically found in AIRE-deficient patients. In addition, 9 months after bone marrow transplantation, Patient 1 developed Hashimoto thyroiditis suggesting that organ-specific autoimmunity may be linked to non-hematopoietic cells such as AIRE-expressing thymic epithelial cells.

Conclusion

Deficiency of DNA-PKcs, a key AIRE partner, can present as an inflammatory disease with organ-specific autoimmunity, thus suggesting a role for DNA-PKcs in regulating autoimmune responses and maintaining AIRE-dependent tolerance in humans.

Key Messages:

DNA-PKcs is a multifunctional protein involved in AIRE-dependent transcription in the thymus. *PRKDC* mutations can lead to a broad range of diseases from severe combined immunodeficiencies to milder immunodeficiency with granulomatous and autoimmune manifestations with positive anti-tissue autoantibodies.

Capsule Summary:

- DNA-PKcs deficiency can be associated with inflammatory granulomatosis mimicking systemic disease.
- Lymphopenia and organ-specific autoantibodies are associated with DNA-PK deficiency.
- Bone marrow transplantation cures the immunodeficiency but might not resolve the AIRE-dependent autoimmunity.

Key words: Autoimmune Regulator (AIRE), Tolerance, DNA-PKcs, *PRKDC*, autoimmunity, VDJ recombination, Severe combined immunodeficiency, RAG

Abbreviations:

DNA-PKcs : DNA-dependent protein kinase catalytic subunit

DSB : Double-Strand Break

CaSR : anti-Calcium Sensing Receptor

SCID : Severe Combined Immunodeficiency

OS : Omenn Syndrome

NK : Natural Killer

AIRE : AutoImmune REgulator

mTEC : Medullary Thymic Epithelial Cell

APECED : Autoimmune PolyEndocrinopathy, Candidiasis and Ectodermal Dystrophy

PBMC : Peripheral Blood Mononuclear Cell

ANA : AntiNuclear autoAntibodies

PCR : Polymerase Chain Reaction

SNP : Single Nucleotide Polymorphism

144

145

Introduction:

Severe combined immunodeficiency (SCID) is the most profound phenotype among the primary immunodeficiencies, occurring secondary to mutations in genes affecting lymphocyte development or function[1]. Children with SCID present with high susceptibility to bacterial, viral and fungal infections in early infancy, and are subject to opportunistic infections, frequently associated with protracted diarrhea and failure to thrive. In the absence of hematopoetic stem cell transplantation or gene therapy, the disease is usually lethal within the first year of life.

Over 20 different genetic deficiencies have been reported with a SCID phenotype, including genes involved in V(D)J recombination, i.e. antigen receptor gene rearrangement (*RAG1, RAG2, DCLRE1C, PRKDC, LIG4, Cernunnos*)[2]. Typically, SCID patients have a severe reduction or absence of circulating T cells and, depending on the causative gene, B cells and natural killer (NK)-cells may also be low or absent.

Whereas null mutations of SCID-related genes cause typical (classical) SCID, hypomorphic mutations are associated with residual T cell differentiation and function and result in atypical (leaky) SCID [2,3]. One such well-described phenotype is Omenn syndrome (OS), comprising early-onset generalized erythroderma (before age 1 year), failure to thrive, diarrhea, hepatosplenomegaly, eosinophilia and increased IgE[4]. In most cases of OS, there is residual function of proteins involved in V(D)J recombination[4,5]. Later-onset, milder forms of primary immunodeficiencies can also occur and are characterized by recurrent infections, autoimmunity and granuloma[6,7,8]. Interestingly, atypical SCID patients with a T^{low} B^{low} phenotype were demonstrated to be more prone to immune dysregulation, including the development of granuloma, autoimmune cytopenia and inflammatory bowel disease[2].

In the context of OS, or T^{low} B^{low} SCID i.e. SCID with autoimmunity and granuloma, distinct mechanisms may jointly contribute to the disruption of immune tolerance. First, a break in both central and peripheral B cell tolerance has been identified in some cases. As an example, in a homozygous *RAG1 S723C* mouse model, V(D)J recombination activity is reduced but not abrogated, and is associated with autoantibody production and expansion of immunoglobulin secreting cells[9]. In this model, the efficiency of B-cell receptor (BCR) editing, a mechanism allowing the rearrangement of the BCR to reduce its autoreactive specificity, is decreased, and the serum level of B cell activation factor BAFF (a key cytokine involved in activation and survival of B cells) is markedly elevated[9]. Secondly, impaired intrathymic T cell maturation has been identified. The Autoimmune Regulator (AIRE) protein is a transcriptional factor expressed in medullary thymic epithelial cells (mTEC) playing a critical role in central T cell tolerance. AIRE induces ectopic expression of autoantigens in mTEC, and drives the negative selection of autoreactive T cells, although the precise molecular mechanisms are still unclear[10,11]. AIRE deficiency leads to the autoimmune polyendocrinopathy, candidiasis and ectodermal dystrophy (APECED) syndrome[11], and is associated with the production of various autoantibodies, including anti-calcium sensor receptor (Anti-CaSR) antibodies in one third of patients[12]. AIRE expression and the development of mTEC are dependent on the presence of positively selected T cells[13,14,15]. A decrease in T cell production may account for low AIRE expression in the thymus[16]. In OS, *AIRE* mRNA and proteins are decreased in patient's thymus and peripheral blood mononuclear cells (PBMC), leading to the suggestion of an impairment in central tolerance[17]. However, no evidence for AIRE-related autoantibodies has been found so far in these patients.

195 *PRKDC* encodes DNA-dependent protein kinase catalytic subunit (DNA-PKcs) which
196 is active when in a hetero-trimeric complex (DNA-PK) with Ku proteins 70 and 80 and
197 in interaction with DNA or RNA[18]. The main function of DNA-PK is to recognize
198 double-strand DNA breaks and to catalyze a repair process known as non-
199 homologous end joining. In a similar way, DNA-PK is crucial for V(D)J recombination
200 in developing T and B cells. Concordantly, DNA-PKcs or Ku deficient mice are
201 severely immunodeficient, with elevated radiosensitivity and susceptiblity to tumour
202 development[19,20]. Besides its role in DNA recombination, DNA-PK has been recently
203 identified in mice as part of a multi-protein complex required for AIRE-dependent
204 expression of peripheral tissue antigens in medullary thymic epithelial cells (mTECs),
205 a process necessary for the establishment of central tolerance[21].
206 Previously, two unrelated typical SCID patients were identified, both with mutations in
207 *PRKDC*[22,23]. The patients presented with a T-B-NK+ phenotype, a failure to thrive
208 and chronic infections during the first year of life. One of them also demonstrated
209 growth failure, microcephaly and seizures[22]. Here, we describe two unrelated
210 patients with *PRKDC* mutations presenting with immunodeficiency and autoimmunity.
211 Both patients had granulomas and a variety of autoantibodies. In addition to an
212 oligoclonal T cell repertoire, these two patients exhibited a progressive T and B cell
213 deficiency and immune dysregulation with a shift to Th1, Th2 but not Th17
214 lymphocytes upon activation. We show that *PRKDC* mutations are responsible for a
215 defect of AIRE transcriptional activity *in vitro*, and are associated with APECED-
216 related autoantibody production.

217 **Results**

218 ***Clinical features of two CID patients.***

This male patient 1 (Pt1) was born to a consanguineous couple of Turkish background (Figure 1A). A younger non-identical twin brother died in the first year of life with a diagnosis of aspiration pneumonia, chronic diarrhea and failure to thrive. At birth, Pt1 was unremarkable with normal weight and occipito-frontal head circumference. He was diagnosed with persistent asthma in the first two years of life and experienced occasional ear infections. At the age of six years, he presented with an acute arthritis involving the left elbow and right knee with positive antinuclear autoantibodies (ANA) (Figure 1B) indicative of an oligoarticular juvenile idiopathic arthritis. He responded well to intraarticular steroid injections and methotrexate. However, secondary to poor methotrexate tolerance (recurrent pneumopathy) this treatment was discontinued. At the 8 years of age, he was diagnosed with bronchiectasis, splenic granuloma (Figure 1C) and skin granuloa (Figure 1D, Figure 1E). Periodic Acid Schiff and Ziehl-Neelsen staining revealed no pathogens (data not shown). Polymerase chain reaction (PCR) assays for *Mycobacteria* and 16s RNA were negative and a diagnosis of sarcoidosis was suggested. Initial T and B cell counts were normal, with increased serum immunoglobulins (Ig) (Table 1). Overtime, Immunoglobulin subclass assessment revealed a deficiency in IgA, IgG2 and IgG4. A decrease in T and B cell numbers was also observed, whereas NK cells remained within normal range. Strikingly, memory phenotype $CD4^+CD45RO^+$ T cells represented more than 90% of circulating CD4 T cells, and $CD4^+CD45RA^+$ T cells were decreased to less than 5%. Immunoglobulin subclass analysis revealed a deficiency in IgA, IgG2 and IgG4, whereas the level of total IgG was increased. Maternal engraftment of T cells was ruled out by PCR (data not shown), and a diagnosis of combined immunodeficiency (CID) with autoimmunity and granuloma was made. After myeloablative conditioning with fludarabin and busulfan, Pt1

underwent bone marrow transplantation from his HLA-identical mother, which resulted in a reconstitution with 100% donor chimerism of the myeloid, B and T cell compartments. Nine months after transplantation his skin granuloma had disappeared. However, concomitant with donor T cell expansion, symptomatic Hashimoto thyroiditis appeared with fatigue, sensititvity to cold, low cardiac rate and increased Thydroid Stimulating Hormone, positive anti-thyroid peroxydase (>300UI/ml) and anti-thyroglobulin (>3000UI/ml) antibodies. Thyroxin substitution was started.

An unrelated female (Pt2) was born to a non-consanguineous couple of Turkish background (Figure 1F). Familial history revealed four deaths in the first two years of life attributed to prematurity (II.4 & II.5) or sepsis (II.6 & II.7). She presented with a history of recurrent lung infections. Bronchiectasis was recognized at the age of 5 years, and splenic granulomatous lesions were identified at 9 years of age on an abdominal CT scan (Figure 1G). Splenic biopsies revealed well-circumscribed caseating epithelioid granulomas with negative special stains for microorganisms (Figure 1H). At the age of 20 years she developed a symmetrical polyarthritis (elbow and knee) sensitive to non-steroidal anti-inflammatory drugs. Immunological assessment revealed low numbers of circulating T and B cells and normal T cell proliferation with mitogen and antigens. (Table 1). IgG levels were increased to over 22g/L, with a monoclonal gammopathy (IgG2k2) even though circulating B cells were undetectable. NK cell count was normal defining a TlowB-NK+ CID. ANA autoantibodies were also detected in the serum of Pt2.

PRKDC mutations are present in both CID patients.

Mutations in *RAG1* and *RAG2* were excluded by Sanger sequencing. Using Single Nucleotide Polymorphism (SNP) analysis in Pt1, and predicting an autosomal recessive pattern of inheritance, a homozygous locus encompassing *PRKDC* was identified on chromosome 8. Sanger sequencing identified a c.9239T>G (p.Leu3061Arg) homozygous missense variant and a homozygous c.6340delGAG (pGly2113del) deletion in *PRKDC* in this patient (Figure 1I). The glycine deletion has an allele frequency of 1% (rs79703138) and has previously been determined as likely non-pathogenic[23]. Conversely, the c9239T>G homozygous variant was predicted as pathogenic on the basis of species conservation, the output of pathogenicity prediction packages (SIFT: deleterious/score: 0, POLYPHEN: probably damaging/score: 1) and their absence from dbSNP, 1000 Genomes project databases, and 13,006 control chromosomes typed for this allele on the Exome Variant Server. One previous report demonstrated that c9239T>G variant results in decreased Artemis activation, leading to impaired coding joint formation and a defect in recombination[23]. The parents of Pt1 were heterozygous for the two variants. Sequencing of the unrelated patient Pt2 revealed the same two variants in the homozygous state.

Patient fibroblasts are defective in DNA double-strand break (DSB) repair. *Previously, PRKDC* mutations have been associated with a defect in DNA DSB repair[22,23]. We first assessed cell survival following seven days of treatment with the radiomimetic drug phleomycin. Primary fibroblast cells of both patients displayed a dose-dependent defect in survival compared to control fibroblasts. Their survival was similar to radiosensitive CERNUNNOS-deficient cells at a dose of 400ng/mL of phleomycin (Figure 2A). Therefore, we analyzed the DSB repair defect in more detail

293 by counting foci of the DSB marker 53BP1 after irradiation in Pt2 fibroblast. 53BP1
294 foci remained increased at 24h compared to the control (Figure 2B and Figure S1
295 available at www.jacionline.org). Thus, we confirmed earlier findings that cells with
296 *PRKDC* mutations result in defective DNA DSB repair [23].
297
298 ***The T cell receptor Vβ repertoire is limited in patients with PRKDC mutations.***
299 DNA-PKcs is mandatory for V(D)J recombination in mouse, and the two previously
300 described patients with *PRKDC* mutations demonstrated a complete lack of T and B
301 cells[22,23]. By contrast, the two patients reported here presented with circulating T and
302 B cells. We, therefore, investigated the T cell Vβ repertoire in both patients using flow
303 cytometry (18 Vβ families with anomalies in Pt1 and Pt2) (Figure 2C) and quantitative
304 PCR (276 combinations Vβ-J, IMGT nomenclature, in Pt1, Figure 2D) at different
305 time points. Molecular PCR analysis of TRBV-J combinations revealed a poorly
306 diversified peripheral T cell repertoire in Pt1 (Figure 2D), together with commonly
307 overrepresented rearrangements such as TRB V27-J2.3, V19-J2.1, V07-J2.1, V10-
308 J1.4, V07-J2.7, V02-J2.2, V03-J1.3 and V05-J2.7. In Pt2, Vβ29 positive T cells were
309 clonally expanded, while most other Vβ families in both patients were under-
310 represented. These data are consistent with limited V(D)J recombination in both
311 patients. We used Immunoscope technology to analyze the T-cell repertoire of Pt2
312 (Figure 2E). The latter experiment showed a major oligoclonal expansion of Vβ29 T
313 cells.
314
315 ***Patients with PRKDC mutations have increased B cell activating factor (BAFF),***
316 ***inflammatory monocytes, and memory T cells expressing of Th1,Th2 but not***
317 ***Th17 cytokines upon activation.*** Limited data are available on the distribution and

function of residual T cells in CID with autoimmunity and granuloma. Th1 and/or Th17 cytokines are supposed to promote granuloma formation[24]. In both patients, we first explored the expression of, and response to, cytokines in the blood. The expression of six interferon-stimulated genes (*IFI27, IFI44L, IFIT1, ISG15, RSAD2* and *SIGLEC1*) was strongly increased in both patients, thus indicating potent *in vivo* interferon induction (Figure 3A). In addition, the expression of BAFF, TNF-α, IFN-γ mRNA in both patients were upregulated in whole blood cells, similarly to patient with *IFIH1* mutations, a recently identified cause of interferon-driven autoimmunity[25] (Figure 3B). In contrast, IL-17A and IL-6 transcripts remained within the normal range (Supplemental Figure 2A). Consistent with these qPCR data, high levels of BAFF and TNF-α were detected in the sera of Pt1 and Pt2 compared with controls (Figure 3C). After BMT, BAFF level decreased in Pt1 to the level of a patient with hypomorphic mutation in Artemis (Supplemental Figure 2B). IFN-γ was normal in patient's sera. Type-I interferon activity, as measured by a viral cytopathic assay was also found normal in the serum of Pt 2 (data not shown).

Next, we analyzed the frequency of a wide range of immune cell subsets in whole blood by flow cytometry, and assessed intracellular expression of several cytokines in lymphocytes upon stimulation with PMA / ionomycin (Table 1; Figure 3 D-H). The percentage of NK cells and dendritic cells appeared normal in both patients. An increased number of inflammatory $CD14^+CD16^+$ monocytes was detected in patients compared to age-matched controls. $CD4^+$ and $CD8^+$ naive T cells were dramatically reduced in patients, in line with a low thymic output. Interestingly, most $CD4^+CD45RA^+$ T cells, routinely referred to as "naïve T cells", were actually memory T cells with no CCR7 expression, defining the T effector memory with RA^+ (TEMRA) subset (data not shown). Similarly, patient $CD4^+CD39^+$ regulatory T cells did not

express CD45RA, suggesting a defect in the thymic development of natural regulatory T cells (Supplemental Figure 2C, available at www.jacionline.org). Upon stimulation with PMA and ionomycin (5h treatment), the production of Th1-related (IFN-γ and TNF-α), Th2-related (IL-4 and IL-13) or Th17-related (IL-17A) cytokines by blood T cell subsets was measured by intracellular staining (Figure 3D-H). Interestingly, $CD4^+$ and $CD8^+CD45RA^-$ memory T cells of both patients secreted more Th2 cytokines IL-4 and IL-13 than in controls, an observation already reported in OS (Figure 3F, 3G). Th1-cytokine TNF-α, IFN-γ were induced in memory T cells (no difference compared to controls), whereas IL-17A expression was reduced in $CD45RA^-$ T cells, suggesting that Th17 cells do not play a role in the pathogenesis of autoimmunity and granuloma in individuals with *PRKDC* mutations (Figure 3H).

AIRE-dependent peripheral tissue antigen expression is impaired by PRKDC mutations. Recently, in mice, DNA-PK was identified as a direct molecular partner of AIRE in the thymus[21], collaborating with AIRE to induce peripheral tissue antigens transcription by mTEC. We therefore hypothesized that *PRKDC* dysfunction might impair the ability of DNA-PK to promote AIRE transcriptional activity. To test this hypothesis, we analyzed fibroblasts derived from controls, from Pt1 and Pt2, and from a patient displaying a typical SCID phenotype (Pt3) previously reported with the same *PRKDC* mutations[23]. Fibroblasts were transiently transfected with *AIRE* cDNA. In wild type human fibroblasts, we measured the expression of AIRE-dependent (*IGFL-1, ALox12, S100A8*) and AIRE-independent (*PRMT3, CCNH, CXCL10*) transcripts, as identified by Abramson and colleagues[21], by quantitative PCR after confirming that AIRE was expressed in fibroblast by western blot (Figure 4A). *PRMT3, CCNH, CXCL10* expression was not modified after AIRE transfection in

fibroblasts (Figure 4A), whereas *IGFL-1* was strongly increased by 60-fold in wild type fibroblasts. In contrast, *AIRE*-transfected fibroblasts from patients Pt1 and Pt2 had a reduced induction of IGFL1 in comparison to controls (Figure 4B). Similar results were obtained using *AIRE*-transfected fibroblasts from the previously reported SCID patient Pt3 (Figure 4C). Following *AIRE* transfection, S100A8 expression was induced in control fibroblasts, but not in fibroblasts of patients with *PRKDC* mutations (data not shown). Taken together, these data indicate that mutated DNA-PKcs prevent AIRE-dependent transcription.

Patients are positive for autoantibody responses against the CaSR. Since the impairment of AIRE function can lead to autoimmune responses against peripheral tissue antigens, we characterized the pattern of autoantibodies in Pt1 and Pt2. In addition to anti-nuclear autoantibodies, both patients were positive for anti-CaSR autoantibodies (Figure 4D and Figure 4E). However, other tissue-specific autoantibodies (tyrosine hydroxylase, phenylanine hydroxylase, tryptophan hydroxylase and NALP5) and anti-cytokine autoantibodies (IFN-α2A, IFN-ω, IFN-λ1, IL-22, IL-17A and IL-17F) were not detected (data not shown). Anti-CaSR are found at a high prevalence in APECED[10,12,21]. Importantly, seven additional atypical SCID patients with defective V(D)J recombination, granuloma and autoimmunity, who did not have *PRKDC* mutations, were negative for anti-CaSR autoantibodies (Table 2). This suggests that the anti-CaSR autoantibody response is specific to the DNA-PK defect found in Pt1 and Pt2. After bone marrow transplantation of Pt1, anti-CaSR autoantibodies strongly decreased, although immunoblotting demonstrated slight persistent positivity (Figure 4D) and Hashimoto thyroiditis occurred 9 months after bone marrow transplantation with the appearance of donor-T and B cells (Figure 4E).

Discussion

Extending the phenotype of *PRKDC* mutated patients, we report here the cases of two unrelated patients with manifestations of CID with immunodeficiency, granuloma and autoimmunity due to a homozygous p.Leu3061Arg mutation in *PRKDC*. Recurrent infections were documented in both cases but their clinical history did not reveal opportunistic infections. Inflammatory manifestations were prominent in Pt1, who was initially diagnosed with ANA positive juvenile idiopathic oligoarticular arthritis. He subsequently developed skin granuloma and lung involvement, which was considered indicative of sarcoidosis. Pt2 was diagnosed with a combined immunodeficiency at the age of 9 years. There was no obvious neurological involvement in either patient. Pt 2 delivered two healthy children.

Both patients carried the same homozygous pathogenic p.Leu3061Arg variant as the first patient published with a mutation in *PRKDC*[23]. All three patients shared a common Turkish ancestry, suggesting a founder effect for these variants. The first two patients reported with *PRKDC* mutations presented with a typical SCID phenotype including recurrent candidiasis and lower pulmonary infections. Of note, one sibling of Pt1 and four siblings of Pt 2 died early in life from recurrent infections. We did not have access to DNA for these individuals but we speculate that their deaths were related to the same primary immunodeficiency being responsible for a typical SCID. The range of clinical phenotypes strongly suggests that additional factors contribute to the overall severity of the disease. Stochastic events or other(s) modifying gene(s) may impact on the overall manifestation of this deficiency. This is

417 reminiscent of the situation already described of T-B-SCID and OS within the same
418 family harbouring the same *RAG1* mutation[26].
419
420 The hallmark of classical OS is an expansion of autoreactive T cells with an HLA-
421 $DR^+CD45RO^+$ phenotype and an oligoclonal T cell repertoire[4]. In OS, the response of
422 activated T cells is skewed towards a Th2 type and is associated with an increased
423 secretion of IL-4 and IL-5 responsible for an elevated production of IgE and
424 eosinophilia, respectively[27]. Here, in the two patients with *PRKDC* mutations, the
425 production of Th2 cytokines was also slightly increased in memory T cells upon
426 stimulation. Th1 and Th17 cells are recognized to play pivotal roles in autoimmunity
427 and granuloma formation in various inflammatory conditions such as Crohn's
428 disease, juvenile idiopathic arthritis and sarcoidosis[28–30]. Th1 cytokines IFN-γ and
429 TNF-α were increased in whole blood cells at the mRNA and protein level upon
430 stimulation of memory T cells isolated from both the CID patients (similarly to
431 controls). However, upon activation, Th17 cytokines were reduced in memory T cells.
432 We hypothesize that Th1 and Th2 cytokines may drive immunopathology in CID with
433 granuloma and autoimmunity. Unexpectedly, however, neither IFN-γ, nor type-I
434 interferon activity were measureable in Pt2 sera, while whole blood cells displayed a
435 strong interferon signature. This signature may be acquired after intra-tissular
436 activation of T cells or might be secondary to chronic activation of innate pathways in
437 response to environmental antigens[31]. Furthermore, BAFF was increased in both
438 DNA-PKcs-deficient patients and ARTEMIS-deficient patients as reported in
439 hypomorphic RAG patients[9] and may promote autoreactive B cell survival.
440 Interestingly, BAFF is produced by activated monocytes and also promotes Th1-

441 associated inflammation in mice. BAFF and Th1 cytokines may synergize in CID and
442 lead to autoimmunity[32,33].
443 In the context of a recombination defect, there are several overlapping mechanisms,
444 detailed in the introduction, which may lead to autoimmunity. ANA+ arthritis has been
445 identified in other patients with immunodeficiency[34,35] and may be related to the T
446 and B cell developmental defect, impaired BCR editing, repertoire disruption and
447 immune cell cytokine overproduction (such as TNFa and BAFF in Pt1 &Pt2). We
448 think that in the context of *PRKDC* mutation, one additional mechanism should be
449 considered: that is, direct impairment of AIRE-dependent tissue-specific antigen
450 expression could promote APECED-like manifestations. The relevance of
451 interactions between AIRE, which plays a critical role in the negative selection of
452 autoreactive T cells[10,11], and DNA-PK was previously tested using NOD.CB17-
453 Prkdc^{scid} mice, which have an inactive form of DNA-PK[21]. These mice lack mature
454 thymocytes and, therefore, mTECs which depend on thymocyte crosstalk for
455 maturation (23-26). To circumvent this issue, mice were reconstituted with wild-type
456 bone marrow to generate chimeric animals with wild-type lymphocytes and DNA-PK-
457 mutant mTECs. Reconstituted NOD.CB17-Prkdc^{scid} mice, but not control mice,
458 demonstrated reduced transcription of AIRE-dependent genes in mTECs, despite
459 similar levels of AIRE expression. The mice also developed late-onset autoimmunity
460 characterized by autoantibody production. Overall, the results indicated that DNA-PK
461 expression in mTECs is crucial to AIRE function[21].
462
463 In the context of *PRKDC* mutations, we have shown that AIRE transcriptional activity
464 is directly impaired leading to a decrease in (e.g., IGFL-1), or absence of (e.g.,
465 S100A8), expression of AIRE-dependent peripheral tissue antigens. These findings

466 are associated with the *in vivo* production of anti-CaSR autoantibodies which were
467 absent in five atypical SCID patients with hypomorphic *RAG* mutations and one with
468 *DLCRE1C* (ARTEMIS) mutation with granuloma and autoimmunity. Moreover, Pt1
469 developed Hashimoto thyroiditis, 9 months after transplantation, which is a rare event
470 in the course of bone marrow transplantation but can be sometimes observed.
471 Positivity of GAD antibodies is also uncommon. These organ-specific autoantibodies
472 suggests that mTECs which are not replaced upon bone marrow transplantation,
473 promoted autoimmunity mediated by newly emigrant naïve T cells. Anti-CaSR
474 autoantibodies were also slightly positive after bone marrow transplantation in the
475 same patient, which may also reflect the persistence of central tolerance defect. Two
476 other patients have been reported with *PRKDC* mutations and a SCID phenotype
477 with a complete absence of T and B cells but no autoimmune manifestations. We
478 acknowledge also that organ-specific autoimmunity observed in our patients could be
479 unrelated to the *PRKDC* mutation. One can also speculate that few circulating T
480 and/or B cells are mandatory for the development of such autoimmune features. After
481 bone marrow transplantation of the SCID patient previously reported (Pt3), the last
482 examination did not reveal autoimmune signs. This suggests that the penetrance of
483 AIRE-associated autoimmunity could be incomplete.
484
485 In summary, *PRKDC* mutations in humans can mimic inflammatory disease with
486 autoimmunity and granuloma. In the CID patients described here, increased cytokine
487 expression may contribute to autoimmunity and granuloma. In addition, *PRKDC*
488 hypomorphic mutations prevent AIRE function. Organ-specific autoimmunity may
489 result from the defective interaction of mutated DNA-PKcs and AIRE in the thymus
490 and anti-CaSR may serve as potential biomarker of this condition.

491

492

493

494

495

496

Material and methods

Details of the materials and methods used in this study are provided in the Methods section in this article's Online Repository at www.jacionline.org.

Acknowledgements

We first acknowledge the patients for their participation in this study. We thank Nadia Plantier and ImmunID Technologies for providing the 3D immune repertoire analysis. This work was supported by Hospices Civils de Lyon, Société Francaise de Rhumatologie and INSERM (AB), as well as NIH grant n° CA162804 (DC); CPRIT RP110465 (DC), INCa_4664 (CC). The T. W. lab is supported by Agence Nationale de la Recherche, European Research council (ERC-Stg 281025), Institut National de la Santé et de la Recherche Médicale (INSERM), Centre National de la Recherche Scientifique (CNRS), Université Claude Bernard Lyon1, ENS de Lyon. YJC acknowledges the European Research Council (GA 309449).

References

1. Fischer A. Human primary immunodeficiency diseases. Immunity 2007;27:835-45.
2. Felgentreff K, Perez-Becker R, Speckmann C, Schwarz K, Kalwak K, Markelj G, et al. Clinical and immunological manifestations of patients with atypical severe combined immunodeficiency. Clin Immunol Orlando Fla 2011;141:73-82.
3. Shearer WT, Dunn E, Notarangelo LD, Dvorak CC, Puck JM, Logan BR, et al. Establishing diagnostic criteria for severe combined immunodeficiency disease (SCID), leaky SCID, and Omenn syndrome: The Primary Immune Deficiency Treatment Consortium experience. J Allergy Clin Immunol 2013;
4. Villa A, Notarangelo LD, Roifman CM. Omenn syndrome: inflammation in leaky severe combined immunodeficiency. J Allergy Clin Immunol 2008;122:1082-6.
5. De Villartay J-P. V(D)J recombination deficiencies. Adv Exp Med Biol 2009;650:46-58.
6. Schuetz C, Huck K, Gudowius S, Megahed M, Feyen O, Hubner B, et al. An immunodeficiency disease with RAG mutations and granulomas. N Engl J Med 2008;358:2030-8.
7. Grunebaum E, Bates A, Roifman CM. Omenn syndrome is associated with mutations in DNA ligase IV. J Allergy Clin Immunol 2008;122:1219-20.
8. Ege M, Ma Y, Manfras B, Kalwak K, Lu H, Lieber MR, et al. Omenn syndrome due to ARTEMIS mutations. Blood 2005;105:4179-86.
9. Walter JE, Rucci F, Patrizi L, Recher M, Regenass S, Paganini T, et al. Expansion of immunoglobulin-secreting cells and defects in B cell tolerance in Rag-dependent immunodeficiency. J Exp Med 2010;207:1541-54.
10. Anderson MS, Su MA. Aire and T cell Development. Curr Opin Immunol 2011;23:198-206.
11. Mathis D, Benoist C. Aire. Annu Rev Immunol 2009;27:287-312.
12. Gavalas NG, Kemp EH, Krohn KJE, Brown EM, Watson PF, Weetman AP. The

calcium-sensing receptor is a target of autoantibodies in patients with autoimmune polyendocrine syndrome type 1. J Clin Endocrinol Metab 2007;92:2107-14.
13. Irla M, Hugues S, Gill J, Nitta T, Hikosaka Y, Williams IR, et al. Autoantigen-specific interactions with CD4+ thymocytes control mature medullary thymic epithelial cell cellularity. Immunity 2008;29:451-63.
14. Surh CD, Ernst B, Sprent J. Growth of epithelial cells in the thymic medulla is under the control of mature T cells. J Exp Med 1992;176:611-6.
15. Poliani P, Vermi W, Facchetti F. Thymus microenvironment in human primary immunodeficiency diseases. [Miscellaneous Article]. Curr Opin Allergy Clin Immunol Dec 2009 2009;9:489-95.
16. Poliani PL, Facchetti F, Ravanini M, Gennery AR, Villa A, Roifman CM, et al. Early defects in human T-cell development severely affect distribution and maturation of thymic stromal cells: possible implications for the pathophysiology of Omenn syndrome. Blood 2009;114:105-8.
17. Cavadini P, Vermi W, Facchetti F, Fontana S, Nagafuchi S, Mazzolari E, et al. AIRE deficiency in thymus of 2 patients with Omenn syndrome. J Clin Invest 2005;115:728-32.
18. Zhang S, Schlott B, Görlach M, Grosse F. DNA-dependent protein kinase (DNA-PK) phosphorylates nuclear DNA helicase II/RNA helicase A and hnRNP proteins in an RNA-dependent manner. Nucleic Acids Res 2004;32:1-10.
19. Blunt T, Gell D, Fox M, Taccioli GE, Lehmann AR, Jackson SP, et al. Identification of a nonsense mutation in the carboxyl-terminal region of DNA-dependent protein kinase catalytic subunit in the scid mouse. Proc Natl Acad Sci U S A 1996;93:10285-90.
20. Gu Y, Seidl KJ, Rathbun GA, Zhu C, Manis JP, van der Stoep N, et al. Growth retardation and leaky SCID phenotype of Ku70-deficient mice. Immunity 1997;7:653-65.
21. Abramson J, Giraud M, Benoist C, Mathis D. Aire's partners in the molecular control of immunological tolerance. Cell 2010;140:123-35.
22. Woodbine L, Neal JA, Sasi N-K, Shimada M, Deem K, Coleman H, et al. PRKDC mutations in a SCID patient with profound neurological abnormalities. J Clin Invest 2013;123:2969-80.
23. Van der Burg M, Ijspeert H, Verkaik NS, Turul T, Wiegant WW, Morotomi-Yano K, et al. A DNA-PKcs mutation in a radiosensitive T-B- SCID patient inhibits Artemis activation and nonhomologous end-joining. J Clin Invest 2009;119:91-8.
24. Torrado E, Cooper AM. IL-17 and Th17 cells in tuberculosis. Cytokine Growth Factor Rev 2010;21:455-62.
25. Rice GI, del Toro Duany Y, Jenkinson EM, Forte GMA, Anderson BH, Ariaudo G, et al. Gain-of-function mutations in IFIH1 cause a spectrum of human disease phenotypes associated with upregulated type I interferon signaling. Nat Genet 2014;46:503-9.
26. De Saint-Basile G, Le Deist F, de Villartay JP, Cerf-Bensussan N, Journet O, Brousse N, et al. Restricted heterogeneity of T lymphocytes in combined immunodeficiency with hypereosinophilia (Omenn's syndrome). J Clin Invest 1991;87:1352-9.
27. Schandené L, Ferster A, Mascart-Lemone F, Crusiaux A, Gérard C, Marchant A, et al. T helper type 2-like cells and therapeutic effects of interferon-gamma in combined immunodeficiency with hypereosinophilia (Omenn's syndrome). Eur J Immunol 1993;23:56-60.
28. Miossec P. Interleukin-17 and Th17 cells: from adult to juvenile arthritis--now it is serious! Arthritis Rheum 2011;63:2168-71.
29. Hölttä V, Klemetti P, Sipponen T, Westerholm-Ormio M, Kociubinski G, Salo H, et al. IL-23/IL-17 immunity as a hallmark of Crohn's disease. Inflamm Bowel Dis 2008;14:1175-84.

30. Ten Berge B, Paats MS, Bergen IM, van den Blink B, Hoogsteden HC, Lambrecht BN, et al. Increased IL-17A expression in granulomas and in circulating memory T cells in sarcoidosis. Rheumatol Oxf Engl 2012;51:37-46.
31. Park J, Munagala I, Xu H, Blankenship D, Maffucci P, Chaussabel D, et al. Interferon signature in the blood in inflammatory common variable immune deficiency. PloS One 2013;8:e74893.
32. Scapini P, Hu Y, Chu C-L, Migone T-S, Defranco AL, Cassatella MA, et al. Myeloid cells, BAFF, and IFN-gamma establish an inflammatory loop that exacerbates autoimmunity in Lyn-deficient mice. J Exp Med 2010;207:1757-73.
33. Sutherland APR, Ng LG, Fletcher CA, Shum B, Newton RA, Grey ST, et al. BAFF Augments Certain Th1-Associated Inflammatory Responses. J Immunol 2005;174:5537-44.
34. Romberg N, Chamberlain N, Saadoun D, Gentile M, Kinnunen T, Ng YS, et al. CVID-associated TACI mutations affect autoreactive B cell selection and activation. J Clin Invest 2013;123:4283-93.
35. Andrès E, Limbach FX, Kurtz J-E, Kurtz-Illig V, Schaeverbeke T, Pflumio F, et al. Primary humoral immunodeficiency (late-onset common variable immunodeficiency) with antinuclear antibodies and selective immunoglobulin deficiency. Am J Med 2001;111:489-91.

Figure 1 :Clinical features of *PRKDC* patients

Pt1 description with (A) Family tree; (B) Positive antinuclear antibodies ; (C) CT scan showing nodular lung lesions with infiltrate (left panel) and spleen granulomatous lesions (right panel); (D) Skin granulomatous lesion of the limb (left panel) and elbow (right panel); (E) Epithelioid non caseating granulomas from skin biopsies. Pt 2 description with (F) Family tree; (G) Hepatomegaly with splenic granulomatosis (CT scan); (H) Caseating granulomas from spleen biopsies, (I) Schematic representation of the DNA-PKcs protein and the mutations as identified in Pt1 and 2.

Figure 2 : DSB repair defect and TCR oligoclonal repertoire

(A) Clonogenic survival assays in control, Cernunnos-deficient, Pt1 and Pt2 fibroblasts. (B) Numbers of γ-53BP1 foci/nucleus following irradiation in Ctl, Pt2 and Cernunnos-deficient fibroblasts (****, $p<0.0001$). (C) Quantitative analysis of Vß distribution in CD3+T cells. Vß under-representation (asterisks) or over-representation (arrows). (D) 3D graph of immune combinatorial diversity in Pt1. (E) Immunoscope of Vß repertoire for Ctl and Pt2.

Figure 3 : Cytokine expression in whole blood and upon activation in T cells

(A) RT-PCR of a panel of six ISG (Mean +/-S.D.) and, (B) RT-PCR of a panel of three cytokines in whole blood. (C) BAFF, IFNγ and TNFα measurement in sera of pediatric or adult Ctl (pCtl, aCtl), Pt1 and Pt2 (D, E, F, G, H) Cytokine expression in both CD4 & CD8 T cells, negative for CD45RA, measured by FACS.

Figure 4 : PRKDC mutations prevent AIRE-dependent IGFL-1 expression.

(A) RT-PCR analysis of 5 transcripts after AIRE transfection in Ctl fibroblasts.(B) and AIRE-dependent IGFL-1 expression in Pt1 and Pt2 (B) or in the previously reported PRKDC mutant with SCID (Pt3) (C), (D) Detection of anti-CaSR autoantibodies in positive and negative control sera and Pt 1 serum, (E) Autoimmune markers in Pt1 before and after BMT

Material and methods

Immunohistochemical analyses. Morphological studies of skin and spleen biopsies were carried out on 5 µm- thick, formalin-fixed, paraffin-embedded samples with hematoxylin and eosin (H&E) staining.

Clonogenic survival assays. 10^4 fibroblasts from healthy control, Cernunnos deficient patient or Pt1 and Pt2 were plated in duplicate on day 0 in culture medium. Increasing dose of the radiomimetic drug phleomycin (Invivogen, Toulouse, France, Grenoble, France) was added and cells were cultured for 7 days. We measured cell number by flow cytometry and analysed the percentage of surviving cells as the ratio of treated/untreated cells.

Analysis of 53BP1 foci after ionizing radiation. Early passaged primary fibroblasts were cultured on cover slips and X-irradiated (5Gy). 1 or 24 hours after irradiation, cells were washed with PBS, fixed with 4% paraformaldehyde for 15 min and incubated for 20 min with PBS 0.1M glycine. Cells were then permeabilized in 0.5% Triton X-100 in PBS for 15 min. After each step, cover slips were rinsed three times with PBS. Thereafter, cells were incubated for 30 min with PBS-BSA 1% and labeled (30 min) with primary antibodies (Anti-53BP1, Novus Biological). Cells were washed with PBS-BSA1% solution and incubated (30 min) with secondary antibodies (Alexa488 goat F(Ab')2, Molecular Probes). Slides were stained 5 min with 0.1 µg/ml of DAPI and mounted in Fluorsave (Calbiochem). Slides were analyzed by epifluorescence microscopy (Axioplan ZEISS). Images were processed for quantification using ImageJ.

T cell receptor Vβ repertoire analysis. T-cell repertoire diversity was measured using the Human ImmunTraCkeR test (ImmunID Technologies), a technology based on genomic DNA Multi-N-plex qPCR technology[1]. Human T cell receptor Vβ-J rearrangements were documented according to IMGT nomenclature (www.imgt.org). Phenotypic analysis of T-cell Vβ repertoire was performed on whole blood samples using the IOTest Beta Mark® kit (Beckman-Coulter, Villepinte, France) containing 24 monoclonal antibodies (mAbs) identifying ~ 70% of the T cell repertoire. Whole blood cells were stained with PECy5-conjugated CD3, PECy7-conjugated CD4 and each combination of 3 FITC-, PE- and FITC/PE-conjugated anti-Vβ mAbs in 8 sample tubes. Whole blood samples were automatically lysed with IMMUNOPREP® Reagent System, washed and fixed in 0.5% formaldehyde in PBS. 0.5 to $1x10^4$ T cells were acquired on a Cytomics FC500 flow cytometer and data were analysed using CXP analysis software. All reagents and instrument were purchased from Beckman-Coulter. Lymphocytes were first gated according to FSC/SSC parameters and then $CD3^+$, $CD4^+$ and $CD3^+CD4^-$ cells were selected. The proportion of each Vβ family was compared to the minimum and the maximum of each reference value obtained from IOTest Beta Mark® kit related data to evaluate expanded or restricted Vβ families. Expansions or restrictions were defined respectively for values above the maximum or below the minimum reference values of the corresponding family.

Immunoscope quantitative repertoire. Method has been described elsewhere[2]. Briefly, total RNA Miniprep kit (Qiagen, Courtaboeuf, France), and cDNA was synthesized using the SuperScript™ II Reverse Transcriptase (Invitrogen™ by Life Technologies in Carlsbad, California). PCR reactions were carried out by combining a reverse primer and a specific fluorophore-labeled probe for the constant region

(MGB–TaqMan probe) with 1 of 24 primers covering the different TRBV chains. The different human TRBV germline genes can be clustered in 24 families according to their level of homology (IMGT nomenclature). Real-time PCR reactions were subsequently carried out with a final concentrations of 400nmol/L of each oligonucleotide primer, 200nmol/L of the fluorogenic probe, and FastStart Universal Probe Master, Rox (Roche Mannheim, Germany). Thermal cycling conditions comprised TaqDNA Polymerase activation at 95°c for 10min, then subjected to 40 cycles of denaturation at 95°c for 15s, annealing and extension at 60°c for 1min. For all these different reactions, real-time quantitative PCR was then performed on an ABI-7300 system (Applied Biosystems, by Life Technologies in Carlsbad, California). The relative usage of each TRBV family was calculated according to the formula:

$$U\,(BVy) = \sum_{x=1}^{x=24} 2^{(Ct(x)-Ct(y))}$$

Ct(x) is the fluorescent threshold cycle number measured for the BVy family.

For Immunoscope profiles, products were then subjected to run-off reactions with a nested fluorescent primer specific for the constant region for a total of three cycles. The fluorescent products were separated and analyzed using an ABI-PRISM 3730 DNA analyzer. The size and intensity of each band were analyzed with "Immunoscope software"[3], which has been adapted to the capillary sequencer. Fluorescence intensities were plotted in arbitrary units on the *y* -axis, and CDR3 lengths (in amino acids) on the *x* -axis.

Measurement of whole blood cytokine expression. Blood was collected into PAXgene tubes (PreAnalytix, Hombrechtikon, Switzerland) and, after being kept at room temperature for between 2 and 72h, was frozen at -20°C until extraction. Total RNA

was extracted from whole blood with a PAXgene (PreAnalytix) RNA isolation kit. RNA concentration was assessed with a spectrophotometer (FLUOstar Omega, Labtech, Ortenberg, Germany). Quantitative reverse transcription PCR (qPCR) analysis was performed using the TaqMan Universal PCR Master Mix (Applied Biosystems, Paisley, UK), and a cDNA derived from 40ng total RNA. Using TaqMan probes for IFI27 (Hs01086370_m1), IFI44L (Hs00199115_m1), IFIT1 (Hs00356631_g1), ISG15 (Hs00192713_m1), RSAD2 (Hs01057264_m1), SIGLEC1 (Hs00988063_m1), IL-1b (Hs01555410_m1), IL-6 (Hs00985639_m1), TNF□ (Hs99999043_m1), IFN□ (Hs00989291_m1), IL-17A (Hs00174383_m1), and TNFSF13 (BAFF) (Hs00198106_m1). The relative abundance of each target transcript was normalised to the expression level of HPRT1 (Hs03929096_g1) and 18S (Hs999999001_s1), and assessed with the Applied Biosystems StepOne software (version 2.1) and DataAssist software (version 3.01). For each of the six probes, individual (patient and control) data were expressed relative to a single calibrator (control C25). The relative quantification (RQ) for each transcript is equal to $2^{-\Delta Ct}$ i.e, the normalised fold change relative to a control.

BAFF ELISA. BAFF was measured in serum samples using a Human BAFF/BLyS/TNFSF13B Quantikine ELISA Kit (R&D Systems) according to the manufacturer's protocol. BAFF concentration was recorded as pg/ml.

TNFα, IFNγ and Type-I IFN. INFγ and TNFα were measured using Elisa kits (Life Technologies) according to the manufacturer's instructions. IFNγ and TNFα concentrations were recorded as UI/ml and pg/ml respectively. Alpha Interferon is titrated with the use of the cytopathic effect inhibibition assay as described[4]. In this antiviral assay, about 1 unit/ml of interferon is the quantity necessary to produce a

cytopathic effect of 50%. Interferon activity is measured on bovine MDBK cells with vesicular stomatis virus[5]. The units are determined with respect to the WHO international standard for Hu-IFN-Alpha 2b (code 95/566) provided by the National Institute for Biological Standards and Control (Pestka 1986)

Phenotypic analysis on whole blood cells. Briefly, 0.5 to $1x10^6$ whole blood cells were stained with a mixture of fluorochrome-labeled antibodies for each panel for 20 minutes at 4°C, then washed twice in staining buffer (Phosphate Buffer Saline, 2% FBS, 1mM EDTA). Antibodies used for staining are listed in Supplementary Table 1. Erythrocytes were lysed at room temperature for 10 min in the dark with BD Pharmlyse buffer 1X (BD Biosciences, Le Pont de Claix, France). Cells were resuspended in 300µl of staining buffer in the presence of 2µL DAPI (2µg/ml) to exclude dead cells, and all events were acquired on a CANTO-II flow cytometer (BD biosciences). Results were analyzed using FlowJo software v9.6.4 (TreeStar, Inc, Ashland, USA). Monocytes were identified as classical ($CD14^+CD16^-$), activated ($CD14^+CD16^+$) or non classical ($CD14^-CD16^+$). CD4 T cells were identified as naive ($CD3^+CD4^+CD45RA^+CCR7^+$), central memory (TCM) ($CD3^+CD4^+CD45RA^-CCR7^+$), effector memory RA+ ($CD3^+CD4^+$ $CD45RA^+$,$CCR7^-$) or effector memory (TEM) ($CD3^+CD4^+CD45RA^-CCR7^-$). CD8 T cells were identified as naive ($CD3^+CD4^-$ $CD45RA^+CCR7^+$), central memory (TCM) ($CD3^+CD4^-CD45RA^-CCR7^+$), effector memory RA+ (TEMRA) ($CD3^+CD4^-CD45RA^+CCR7^-$) and CD8 effector memory (TEM) ($CD3^+CD4^-CD45RA^-CCR7^-$).

Assessment of cytokine production in activated whole blood cells: Briefly, 900µL of heparinized whole blood was incubated at 37°C in 5% CO2 humidified atmosphere for 5 hours, in the presence or absence of PMA (50ng, Sigma-Aldrich) and ionomycin (1ng/mL, Sigma-Aldrich, Saint Quentin Fallavier, France) together with protein transport inhibitor (GolgiPlug, 10µg/mL, BD biosciences). At the end of the stimulation, erythrocytes were lysed at room temperature with BD Pharmlyse buffer. White blood cells were washed in staining buffer and stained with the corresponding surface antibodies panel. After washing in PBS, cells were fixed with Formaldehyde (Sigma-Aldrich) at 2% final for 20 minutes at 4°C, then washed twice in staining buffer and stored overnight at 4°C. Cells were then permeabilised in staining buffer supplemented with 0.5% saponine and stained 20 minutes at 4°C with the corresponding intra-cytoplasmic anti-cytokine antibodies (IL-2, IL-4, IL-13, IL-17, IFNγ, TNFα).Cells were resuspended in 600µl of staining buffer and all events were acquired on a flow cytometer fitted with four lasers (violet, blue, yellow and red) (LSRII Fortessa for functional analyses BD biosciences). Results were analyzed using FlowJo software v9.6.4 (TreeStar, Inc) and cytokine secretion by different cell subsets defined by the gating strategy was evaluated by creation of Boolean gates.

Fibroblast transfection and immunoblotting to detect AIRE expression.: Primary fibroblasts were cultured from a skin biopsy sample from patients 1, 2 or a control in DMEM supplemented with 10% fetal bovine serum, 2mM glutamine, 10mM Hepes and 40µg/ml gentamycin (Life Technologies, Courtaboeuf, France). Fibroblasts were transfected either with pMax-GFP (Lonza, Basel, Switzerland) vector or with TrueORF gold vector coding for Myc-DDK-tagged ORF of human AIRE transcript variant AIRE-1 (OriGene Technologies, Rockville) using the jetPEI reagent (Polyplus transfection, Illkirch, France). After 24 hours, fibroblasts were lysed in NP40 lysis

buffer (20mM Tris, HCl pH7.4 ; 150mM NaCl ; 2mM EDTA ; 1% NP40) containing protease inhibitors for 30min at 4°C. Supernatant was collected following 10min centrifugation at 16 000g, 4°C and protein content was quantified using µBCA quantification kit (Thermo Fisher Scientific Biosciences, Villebon sur Yvette, France). Protein extract (50µg) were analysed by western blot using anti-AIRE antibody (Abnova, Tapai, Taiwan), anti-rabbit IgG antibody conjugated to horseradish peroxidase (1:10,000) (Sigma-Aldrich), and a BM Chemiluminescence Blotting Substrate Kit (Roche).

Measurement of gene expression in AIRE-transfected fibroblasts. Fibroblasts from patients or controls were cultured and transfected as above. After 24h hours, total RNA was extracted using TRIzol® reagent according to manufacturer's instructions (Life Sciences). Quality and absence of genomic DNA contamination were assessed with a Bioanalyzer (Agilent, Massy, France). We used High capacity RNA-to-cDNA kit (Applied Biosystem, Carlsbad, USA) to generate cDNA for RT-PCR. PCR was carried out with a SybrGreen-based kit (FastStart Universal SYBR Green Master, Roche, Basel, Switzerland) on a StepOne plus instrument (Applied biosystems, Calrlsbad, USA). Primers were designed using the Roche website (Universal ProbeLibrary Assay Design Center) (IGFL-1: forward : 5'-GGCTGCATCGTAGCTGTCTT-3'; reverse : 5'-GCATCAGGTAAGGAGTCATGG-3' ; Alox12 : forward :5'-CTGAAGATGGAGCCCAATG-3' ; reverse : 5'-ACAGTGTTGGGGTTGGAGAG-3' ; PRMT3 : 5'-CAGGGTCGTGTTCTCTACGG-3' ; reverse : 5'- TTTCCTTTCAAGGCTTCACCT-3'; CCNH : forward 5'-ATGATTACGTCTCAAAGAAATCCA-3' ; reverse : 5'-CTACCAGGTCGTCATCAGTCC-3' ;CXCL10 : forward : 5'-

GAAAGCAGTTAGCAAGGAAAGGT-3' ; reverse : GACATATACTCCATGTAGGGAAGTGA-3' ; OAZ1 : forward : 5'-GGATAAACCCAGCGCCAC-3' ; reverse : 5'-TACAGCAGTGGAGGGAGACC-3').

Detection of autoantibodies against the CaSR: The immunoblotting method for detecting anti-CaSR autoantibodies is described elsewhere[6]. Briefly, 20-µg samples of *Escherichia coli*-expressed CaSR extracellular domain (amino acid residues 1 to 603; SWISS-PROT nr. P41180) were separated by SDS-PAGE and transferred to nitrocellulose membrane. Membranes were used in standard immunoblotting experiments with patient or control sera (1:100 dilution), anti-human IgG antibody conjugated to horseradish peroxidase (1:2,000 dilution) (Sigma-Aldrich), and a BM Chemiluminescence Blotting Substrate Kit (Roche). In addition, anti-CaSR autoantibodies were detected in some patient serum samples using a CaSR immunoprecipitation assay as detailed previously[7].

Detection of anti-nuclear autoantibodies (ANA): The method has been described elsewhere[8]. Briefly, the detection was performed by indirect immunofluorescence technique (IIF) using HEp2 cells. Sera diluted at 1:160 were incubated on HEp2 cells (Biorad, Marnes la Coquette, France) for 30 min at room temperature. After 3 washes in phosphate buffer saline (PBS) pH 7.4, the slides were incubated with a goat anti-human IgG ($F(ab')_2$) FITC-conjugated to fluorescein isothiocyanate (diluted at 1:100) (Biorad) for 30 min at room temperature. The slides were examined using an Olympus fluorescence microscope. A classical titration of each ANA positive at a titer of 1:160 was performed by serial 1 in 2 dilution until 1:1280. A titer equal or greater than 1:160 was interpreted as a positive result.

*Statistical analyses.*Differences in numbers of foci were analyzed using the nonparametric Mann-Whitney U test (1-tailed; $P < 0.05$ was considered significant) in the GraphPad Prism program (GraphPad Software).

Study approval. The study was approved by the Medical Ethics Committee of Sud Est III, Lyon, France, and was carried out in accordance with the Declaration of Helsinki principles. All patients provided written informed consent for inclusion of their details and samples in the study.

Supplemental Figure 1 :
53BP1 Foci after X-ray irradiation of Pt2fibroblasts. Time points 1h, 24h.

Supplemental Figure 2 :
(A) Quantitative reverse transcription PCR of a panel of 3 cytokines in whole blood measured in Pt1 (before BMT) and Pt2 and 29 controls (Mean +/-S.D.). (B) B cell activating factor (BAFF) measurement in sera of Pt1 (Pre and Post BMT) and Pt2, one Artemis-deficient patient and 6 controls by ELISA. (C) CD39 expression in TReg cells (CD4+CD25+CD127low) in Pt 1 (Pre-BMT) and Pt2 compared to age matched control (pCtl : pediatric Ctl ; aCtl : adult Ctl).

Figure No 1
Click here to download Figure No 1 Figure1.eps

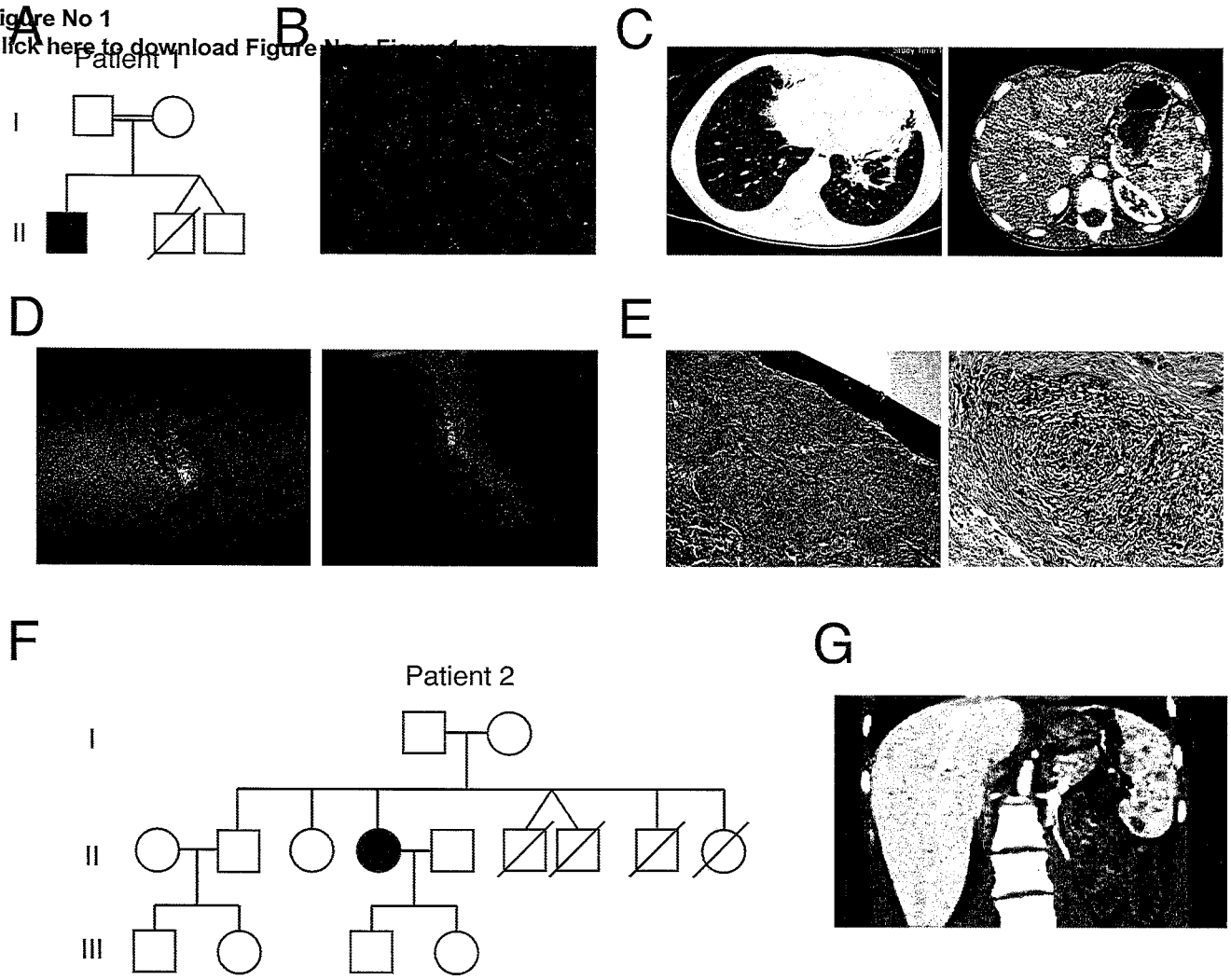

Mathieu et al, Figure 1

Figure No.2
Click here to download Figure No.: Figure2.eps

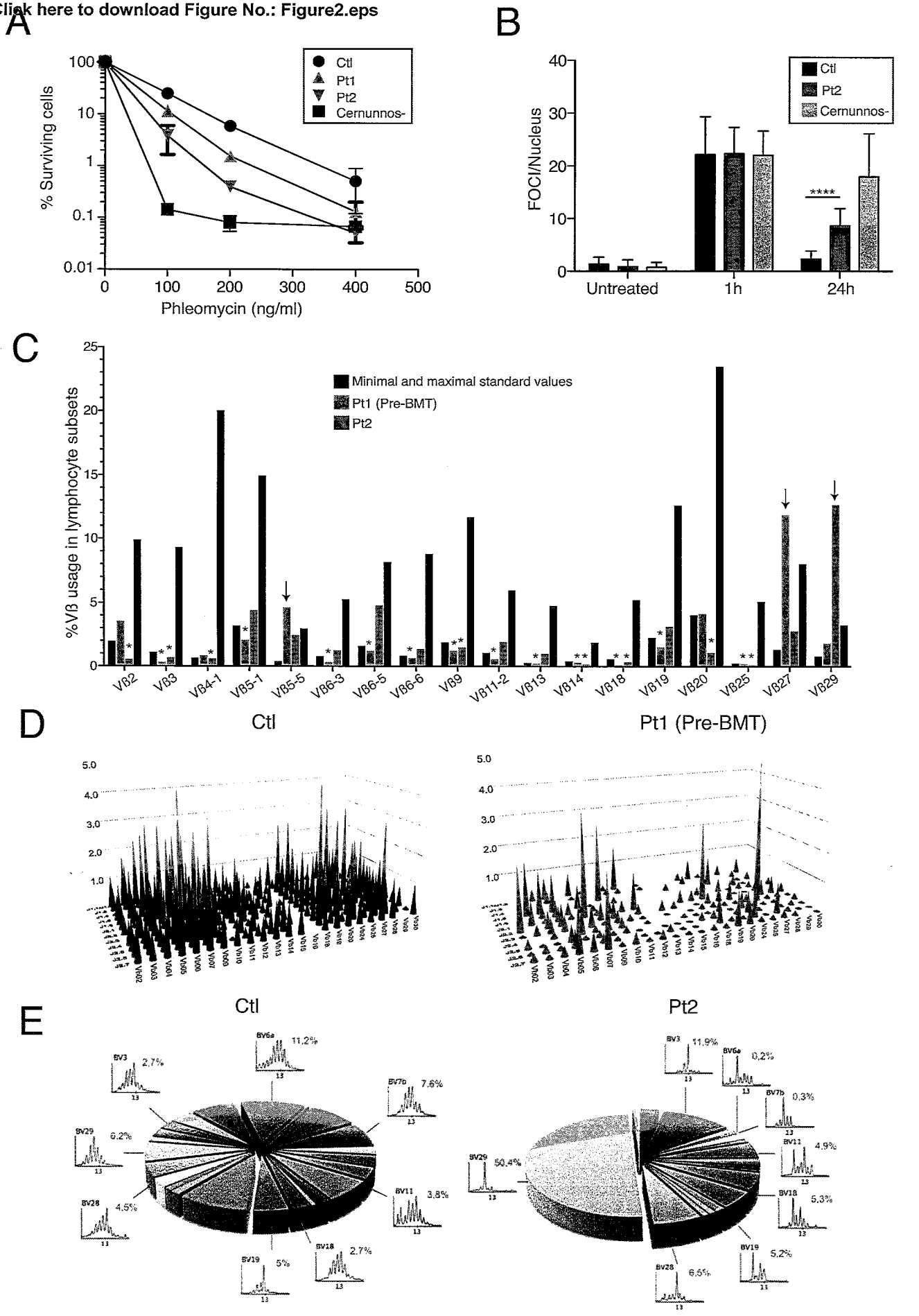

Mathieu *et al.*, Figure 2

Figure No.3
Click here to download Figure No.: Figure3.eps

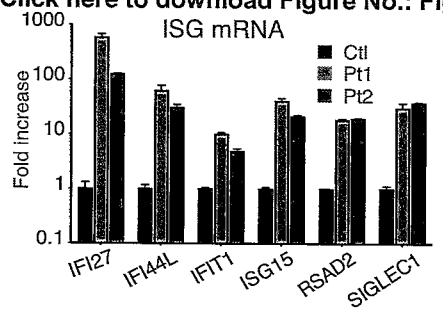

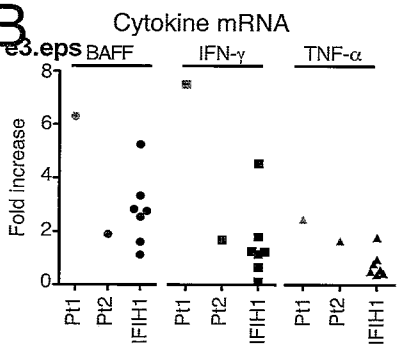

C

	Ctl	Pt1	Pt2
BAFF (pg/ml)	340	12285	13094
IFNγ (UI/ml)	<0,2	<0,2	<0,2
TNFα (pg/ml)	<15	83	47

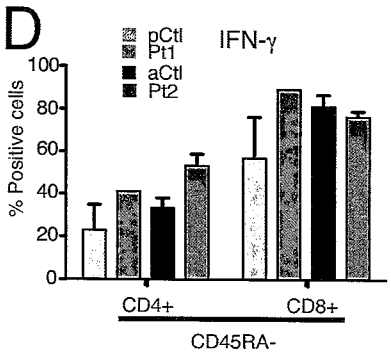

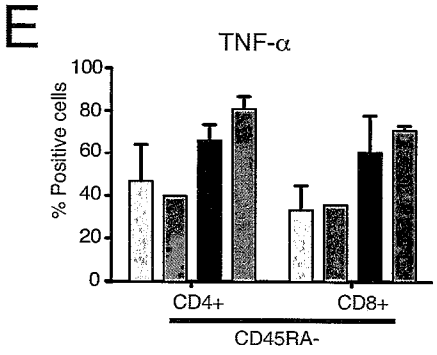

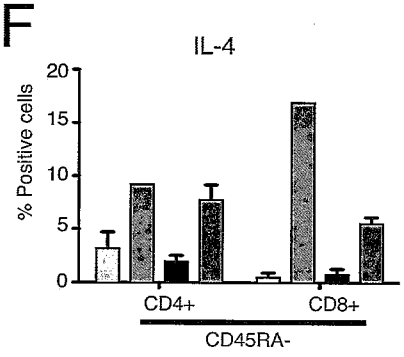

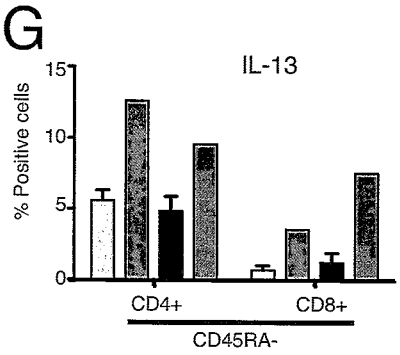

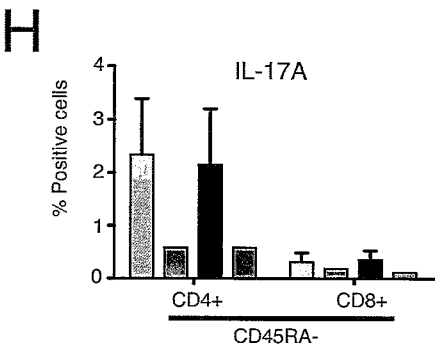

Figure No.4
Click here to download Figure No.: Figure4.eps

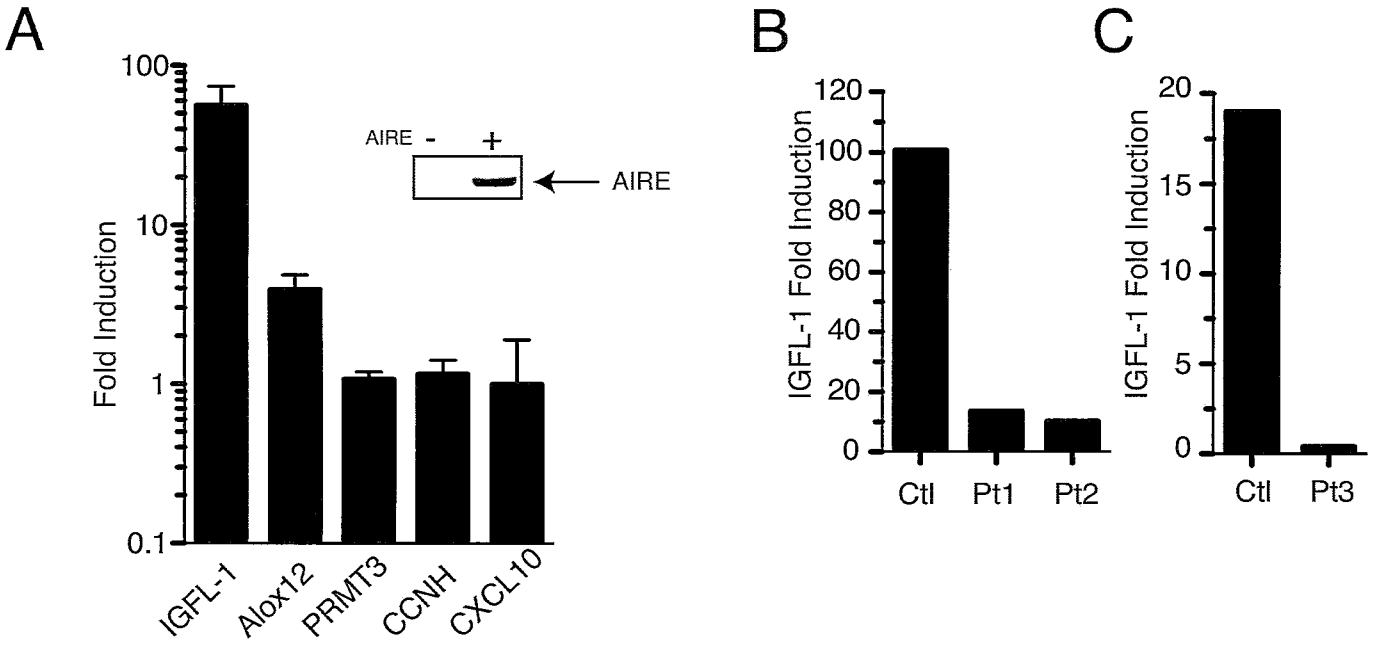

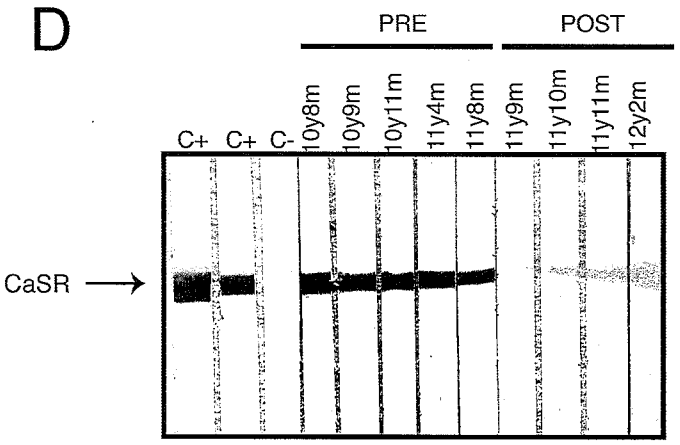

E

Time to HSCT (Months)		-3 M	+2 M	+9 M
Age		11y4m	11y9m	12y6m
Autoimmune manifestations		None	None	Grave's disease
T cell count (G/L)		1,1	1,6	2,4
Chimerism			100%	100%
Auto antibodies	**CaSR**	**pos+++**	**pos**	**low pos**
	thyrglobulin <60	21	18	**>3000**
	TPO <60	8	11	**1890**
	islet	<10	<10	<10
	gad <5	1,8	2,6	**55,3**
	ia2 <10	0,2	1,4	0,8
	transgluA <0,1	<0,1	<0,1	<0,1
	Adrenal <4	<4	<4	<4
	21hydroxy <1.1	0,2	0,6	<0,2
	ANA	**160dot**	<160	<160

Figure No.4
Click here to download Figure No.: Figure4.eps

A

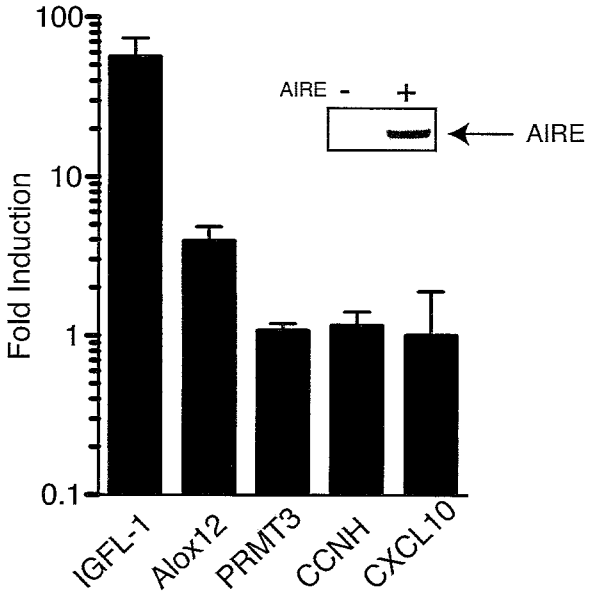

B

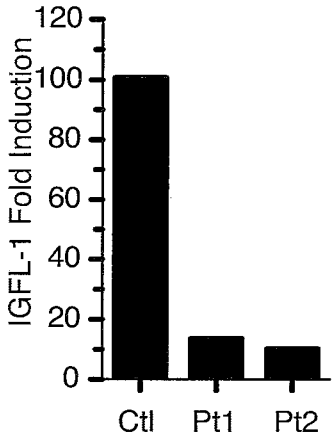

C

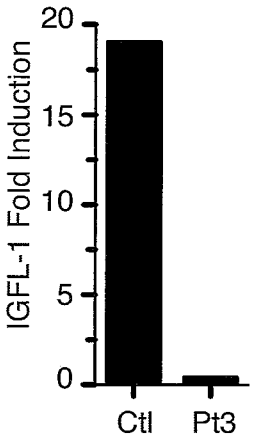

D

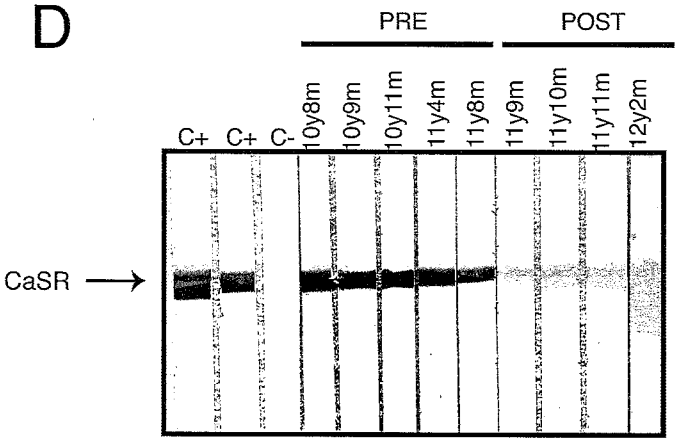

E

Time to HSCT (Months)		-3 M	+2 M	+9 M
Age		11y4m	11y9m	12y6m
Autoimmune manifestations		None	None	Grave's disease
T cell count (G/L)		1,1	1,6	2,4
Chimerism			100%	100%
Auto antibodies	**CaSR**	**pos+++**	**pos**	**low pos**
	thyrglobulin <60	21	18	**>3000**
	TPO <60	8	11	**1890**
	islet	<10	<10	<10
	gad <5	1,8	2,6	**55,3**
	ia2 <10	0,2	1,4	0,8
	transgluA <0,1	<0,1	<0,1	<0,1
	Adrenal <4	<4	<4	<4
	21hydroxy <1.1	0,2	0,6	<0,2
	ANA	**160dot**	<160	<160

Repository E Figure No.1

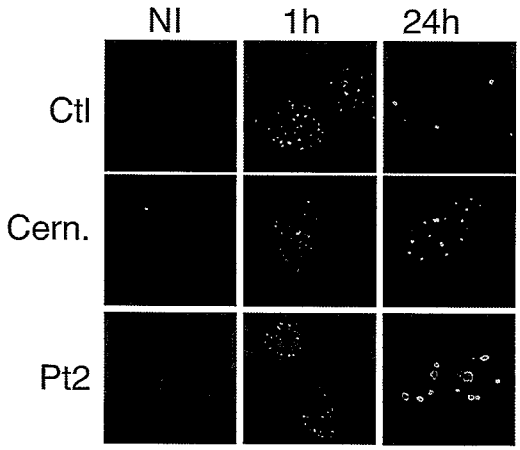

Mathieu et al. Supplemental Figure 1

Repository Figure No.2

A

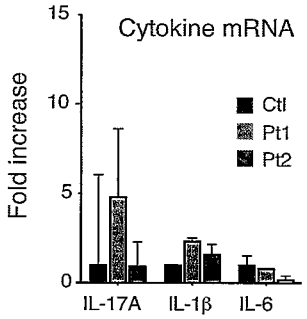

B

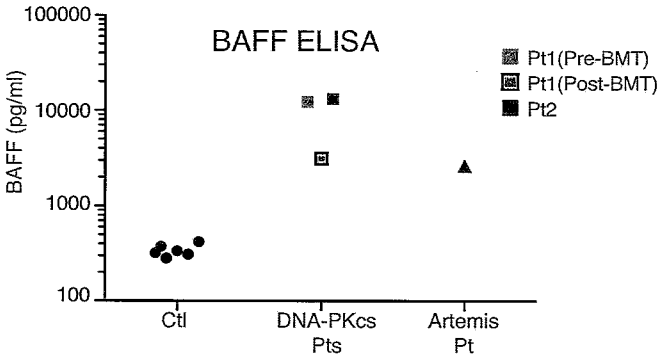

C

	%CD45RA-CD39+	S.D.	%CD45RA+CD39+	S.D.
pCtl	34.05	25.4	6.4	3.2
Pt1	96.8		0.8	
aCtl	35.9	16.1	6.7	3.7
Pt2	89.2		0.06	

		Patient 1 (before BMT)						Patient 2					
		6yo	Normal values /µL (%)	8yo	10yo	11yo	Normal values /µL (%)	14yo	15yo	Normal values /µL	18yo	20yo	Normal values /µL
	Lymphocyte count /µL (%)	**7324 (21)**	2100-6450 (33-62)	**774 (11)**	**1264 (18)**	**668 (13)**	1440-5340 (29-56)	**699 (15)**	**467 (12)**	1400-3300	**890 (32)**	**637 (14)**	1000-4000
	T cell population /µL (%)												
	$CD3^+$	3589 (49)	1350-3900 (56-77)	**387 (50)**	**670 (53)**	**334 (50)**	1060-3370 (59-79)	**433 (62)**	**289 (62)**	1000-2200	**623 (70)**	**376 (59)**	700-2100
	$CD3^+CD4^+$	1245 (17)	740-2450 (27-49)	**186 (24)**	**265 (21)**	**154 (23)**	420-1930 (29-50)	**269 (38)**	**165 (35)**	530-1300	**380 (42)**	**278 (44)**	530-1300
	$CD3^+CD8^+$	**1978 (27)**	500-1610 (19-34)	**194 (25)**	**392(31)**	**180 (27)**	410-138 (20-34)	**91 (13)**	**90 (19)**	390-920	**168 (19)**	**49 (7)**	330-920
	Naive CD4 T cells $CD4^+CD45RA^+$	**50 (4)**	100-800 (66-77)	**2 (1)**	**5 (2)**	**3 (2)**	100-800 (55-67)	**0**	**0**	23-770	**0**	**4 (1)**	23-770
	Memory CD4 T cells $CD4^+CD45RO^+$	1145 (92)	150-850 (NA)	171 (92)	252 (95)	137 (89)	150-850	269 (62)	**182 (63)**	240-700	423 (68)	263 (70)	240-700
	Double negative $CD3^+CD4^-CD8^-$				**1 (0.2)**		9-78 (0.3-1.8)	**17 (2)**	**14 (3)**	9-78 (0.3-1.8)	**19 (3)**	**56 (9)**	7-74 (0.3-1.8)
	Regs $CD3^+CD25^+CD127^-$				**9 (3.4)**	**7 (4.8)**	44-60 (4-10)						
	TCR□□					**311 (93.1)**	150-850 (80-98)						
	TCR□□					22 (6.5)	20-350 (2-14)						
	Natural Killer ($CD16^+CD56^+CD3^-$) /µL (%)	**3442 (47)**	150-800 (6-19)	**364 (47)**	**569 (45)**	**307 (46)**	145-600 (6-21)	231 (33)	149 (32)	70-480	196 (22)	229 (36)	90-600
	Dendritic cells					0.73	0.624-0.853					0.75	0.624-0.853
Monocytes	Classical monocytes ($CD14^+CD16^-$)					**3.64**	472-780					**1.44**	472-780
Monocytes	Inflammatory monocytes ($CD14^+CD16^+$)					**828.61**	18-44					**187.19**	18-44
Monocytes	Non classical monocytes ($CD14^-CD16^+$)					**86.19**	15-39					35.08	15-39
	B cell /µL (%)												
	$CD19^+$	**147 (2)**	370-1570 (15-34)	**8 (1)**	**13(1)**	**7 (1)**	230-1130 (10-27)	**0**	**0**	110-570			
	Immunoglobulin - g/L												
	IgG				**14.6**	**14.1**	6.55-12.17					**22**	6.55-12.17
	IgG1				8.8	**11.5**	4.23-10.6						
	IgG2				**<0.02**	**0.2**	0.76-3.55						
	IgG3				1.159	1.131	0.17-1.73						
	IgG4				**<0.003**	**<0.003**	0.016-1.15						
	IgA				**<0.06**	**<0.06**	0.51-1.63					**<0.06**	0.75-2.38
	IgM				1.29	1.44	0.57-1.62					0.88	0.71-2.02
	IgE					<4.88.10-6	<366.10^{-6}					<4.88.10-6	<366.10^{-6}

Table 1 : Clinicobiological assessment of Pt1 and Pt2

Patient	Mutation	Clinical history	Serum related to HSCT	Age at time of sample	CaSR Ab
Pt1	*PRKDC* p.Leu3062Arg ; p.Leu3062Arg	Arthritis, skin granuloma, reccurent infections	PRE		+ (46.4)
			POST		+ (3.26)
Pt2	*PRKDC* p.Leu3062Arg ; p.Leu3062Arg	Arthritis, spleen granuloma, reccurent infections	PRE		+ (28.1)
Artemis	*DCLRE1C* p.Leu70del ; p.0 (del exons 1–4)	No severe infection Cutaneaous granuloma	PRE	<6yo	-
RAG case 1	*RAG1* p.Arg474Cys ; p.Lys983AsnfsX9	autoimmune cytopenia, severe infections	PRE	2yo	-
			POST	>29mo	-
RAG case 2	*RAG1* p.Arg474Cys ; p.Lys983Asn	autoimmune cytopenia, severe infections	PRE	>8yo	-
RAG case 3	*RAG1* p.Arg841Gln ; p.Phe974Leu	idiopathic T cell lymphopenia, sister with severe autoimmunity	PRE	<3mo	-
RAG case 4	*RAG1* p.His612Arg ; pHis612Arg	Evans sy, skin granuloma, splenomegaly, severe infections	POST	10yo	-
RAG case 5	*RAG1* p.Arg314Trp ; p.Arg507Trp/Arg737His	skin granuloma, EBV lymphoma, no severe infections	PRE	<6yo	-
RAG case 6	*RAG2* p.Phe62Le ; p.Phe62Leu	autoantibodies, T cell lymphopenia, severe infections	PRE	29yo	-

Table 2 : Anti-CaSR assessment in patients with V(D)J recombination deficiency